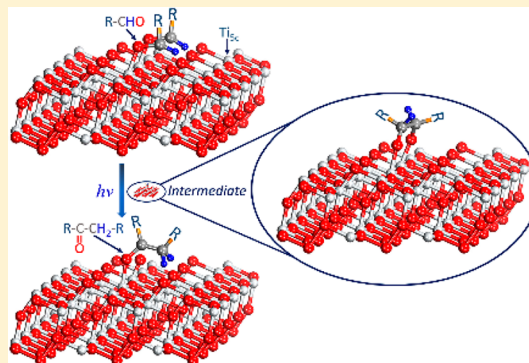


Photoinduced Carbonyl Coupling of Aldehydes on Anatase TiO<sub>2</sub>(101)Zhenhua Geng,<sup>†</sup> Xiao Chen,<sup>†</sup> Wenshao Yang, Qing Guo,<sup>\*</sup> Dongxu Dai, and Xueming Yang<sup>\*</sup>

State Key Laboratory of Molecular Reaction Dynamics, Dalian Institute of Chemical Physics, 457 Zhongshan Road, Dalian 116023, Liaoning, People's Republic of China

## S Supporting Information

**ABSTRACT:** Carbonyl coupling of aldehydes is critical to many synthetic processes, including the development of alternative fuels and useful synthetic chemicals. We report a general photoinduced process for carbonyl coupling of aldehydes as a route to ketone synthesis. In contrast to thermal carbonyl coupling of aldehydes with O<sub>2</sub> to ketones via carboxylate-type intermediates at high temperature, carbonyl coupling of aldehydes (CH<sub>3</sub>CHO, CH<sub>3</sub>CH<sub>2</sub>CHO, PhCHO) to produce ketones on anatase-TiO<sub>2</sub>(101) can be promoted by UV light below room temperature with high efficiency on the Ti<sub>5c</sub> sites, while aldehydes can also be decomposed during UV light irradiation. The mechanistic model constructed in this study elucidates the crucial role of TiO<sub>2</sub> as a photocatalyst for synthetic reactions and provides a new pathway in conversion of aldehydes to ketones.



## ■ INTRODUCTION

Since the discovery of photocatalytic splitting of water on TiO<sub>2</sub> photoelectrode under ultraviolet (UV) light in 1972 by Honda and Fujishima,<sup>1</sup> a great deal of effort has been devoted to the research of TiO<sub>2</sub> materials, which has led to many potential applications in areas ranging from photocatalysis and photovoltaics to thermocatalysis and sensors.<sup>2–9</sup> Recently, there has been a growing research interest in carbon–carbon coupling of aldehydes<sup>10–24</sup> due to interest in biomass conversion to fuels and useful synthetic chemicals, such as olefins and ketones.

The McMurry reaction, aldol condensation, and ketonization are important routes in which aldehydes (or carbonyl containing species) can be converted into longer chain molecules. McMurry reaction of aldehydes usually yields olefins through reductive coupling of aldehydes on reduced TiO<sub>2</sub> surfaces.<sup>11–15</sup> Aldol condensation on TiO<sub>2</sub> is initiated from combination of two molecules of aldehyde to produce  $\beta$ -hydroxyl aldehyde, which is easily dehydrated to form new aldehyde or isomerized to form an olefinic alcohol.<sup>16–24</sup> The 2-butanone product from carbonyl coupling of acetaldehyde (CH<sub>3</sub>CHO) as a main reaction channel is only observed on highly reduced rutile(R)-TiO<sub>2</sub>(110) by Yang and co-workers,<sup>10</sup> whereas ceria-based catalysts are active for ketonization of aldehydes, in which the aldehydes are oxidized to a carboxylate-type species on the surface that then couples to produce the ketones with the evolution of CO<sub>2</sub> and water (H<sub>2</sub>O).<sup>25–27</sup> In early studies, ketonization of carboxylate-type species on TiO<sub>2</sub> with the evolution of CO<sub>2</sub> and H<sub>2</sub>O can be also achieved.<sup>28,29</sup> Compared to ceria-based catalysts, the poor oxygen storage capacity of TiO<sub>2</sub> makes efficient ketonization of aldehydes via carboxylate-type species nearly impossible. However, these studies are focused on the thermal chemistry of aldehydes on TiO<sub>2</sub> surfaces, and ketonization from carbonyl coupling of

aldehydes is rarely observed. Thus, there is interest in photoinduced carbonyl coupling of aldehydes to form ketones without oxygen by using the photocatalytic properties of TiO<sub>2</sub>. In this work, photoinduced ketonization from carbonyl coupling of aldehydes (CH<sub>3</sub>CHO, propionaldehyde (CH<sub>3</sub>CH<sub>2</sub>CHO), benzaldehyde (PhCHO)) on anatase(A)-TiO<sub>2</sub>(101) has been carried out using temperature-programmed desorption (TPD). Our results clearly illustrate that ketones formation via photoinduced carbonyl coupling of aldehydes occurs efficiently on A-TiO<sub>2</sub>(101).

## ■ EXPERIMENTAL METHODS

TPD experiments were carried out in an ultrahigh vacuum (UHV) chamber with a pressure in the low 10<sup>–11</sup> Torr range. Details of the TPD apparatus have been described elsewhere.<sup>30</sup> The A-TiO<sub>2</sub>(101) single crystal was purchased from Princeton Scientific Corp. (6 × 6 × 1 mm<sup>3</sup>). The surface was cleaned by cycles of Ar<sup>+</sup> sputtering and UHV annealing. Daily cleaning was accomplished by annealing the crystal at 800 K for 30 min in UHV. Aldehydes (Sigma-Aldrich, 99%) were purified by several cycles of “freeze–pump–thaw” and then dosed to the sample at 100 K through a home-built calibrated molecular beam doser. A 266 nm ns laser (HIPPO, Spectra-Physics) with a power intensity of 70 mW/cm<sup>2</sup> and a repetition rate of 30 kHz was used in this experiment. Annealing in vacuum at 800 K for 20 min between TPD experiments was performed to heal and clean the surface. TPD signals were collected with a ramping rate of 2 K/s and with the sample facing the mass spectrometer.

Received: March 15, 2016

Revised: April 7, 2016

Published: April 18, 2016



## RESULTS

**Photoinduced Carbonyl Coupling of  $\text{CH}_3\text{CHO}$ .** Before irradiation, TPD spectra of various mass traces with 0.8 ML (1 ML =  $5.2 \times 10^{14} \text{ cm}^{-2}$ ) of  $\text{CH}_3\text{CHO}$ -covered A- $\text{TiO}_2(101)$  surfaces were measured, as shown in Figure 1. Three desorption

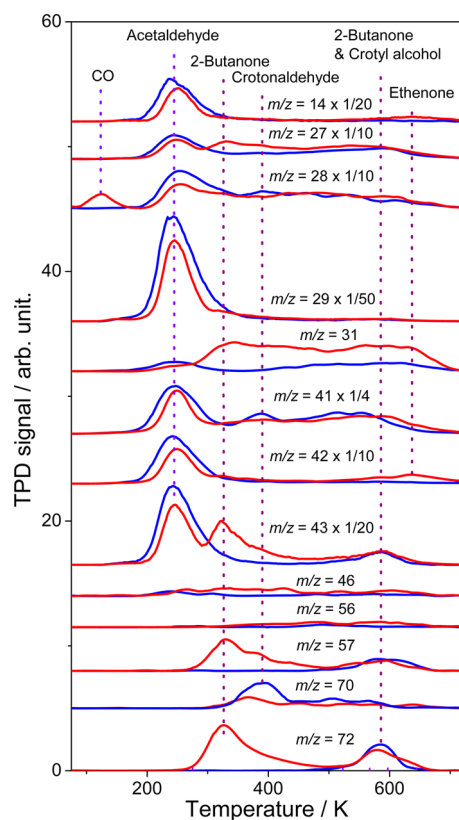


**Figure 1.** TPD spectra acquired at  $m/z = 27$  ( $\text{C}_2\text{H}_3^+$ ), 28 ( $\text{CO}^+$ ,  $\text{C}_2\text{H}_4^+$ ), 29 ( $\text{CHO}^+$ ), 31 ( $\text{CH}_3\text{O}^+$ ), 41 ( $\text{C}_3\text{H}_5^+$ ), 42 ( $\text{C}_2\text{H}_2\text{O}^+$ ,  $\text{C}_3\text{H}_6^+$ ), 43 ( $\text{C}_2\text{H}_3\text{O}^+$ ,  $\text{C}_3\text{H}_7^+$ ), 46 ( $\text{C}_2\text{H}_6\text{O}^+$ ), 56 ( $\text{C}_4\text{H}_8^+$ ), 57 ( $\text{C}_3\text{H}_5\text{O}^+$ ,  $\text{C}_4\text{H}_9^+$ ), 70 ( $\text{C}_4\text{H}_6\text{O}^+$ ), and 72 ( $\text{C}_4\text{H}_8\text{O}^+$ ) after irradiating the 0.8 ML of  $\text{CH}_3\text{CHO}$ -covered A- $\text{TiO}_2(101)$  surface 0 (blue) and 10 min (red).

peaks at 243, 390, and 580 K were observed (blue line). The significant desorption peak at 243 K ( $m/z = 27, 28, 29, 41, 42, 43$ ) is assigned to  $\text{CH}_3\text{CHO}$  desorption from the five coordinated  $\text{Ti}^{4+}$  sites ( $\text{Ti}_{5c}$ ). A recent scanning tunnel microscopy (STM) study by He and co-workers<sup>31</sup> shows that a very low concentration of surface point defects on the A- $\text{TiO}_2(101)$  surface can be formed by vacuum annealing. Thus, no obvious butene product is observed via the self-coupling of two  $\text{CH}_3\text{CHO}$  molecules adsorbed on surface vacancy sites. Based on previous studies of aldol condensation of  $\text{CH}_3\text{CHO}$  on signal-crystal and polycrystalline  $\text{TiO}_2$  surfaces,<sup>14,20</sup> the 390 K peak at  $m/z = 41$  and 70 is due to crotonaldehyde formation, while little signal of the 580 K peak at  $m/z = 31$  (Figure 1) suggests that the TPD peak does not mainly result from crotyl alcohol or other alcohols desorption. Taking into account mass spectrometer sensitivity factors, the 580 K product is identified to be 2-butanone by comparison of the fragmentation pattern of the evolving species to that given in the NIST database. This assignment has been further verified by a separate experiment with a 0.22 ML of 2-butanone-covered A- $\text{TiO}_2(101)$  surface (Figure S1); the respective relative intensities of the 305 K TPD peak for 2-butanone at  $m/z = 43, 57$ , and 72 are

1:0.062:0.098, which are nearly the same with those of the 580 K product (1:0.068:0.102). The higher ratio of  $m/z = 57$  for the 580 K peak product may be due to crotyl alcohol formation, which is also desorbed at 580 K during TPD.

After irradiation, a big desorption peak is observed at 320 K ( $m/z = 27, 43, 57$ , and 72). The respective relative intensities of the 320 K peak at  $m/z = 43, 57$ , and 72 are the same as that of 2-butanone, clearly suggesting that the 2-butanone product is formed during 266 nm irradiation via carbonyl coupling of  $\text{CH}_3\text{CHO}$  on the surface, while the other products, CO (125 K peak at  $m/z = 28$ ) and ethenone (635 K peak at  $m/z = 14, 42$ ), are also observed. Except these products, a broad peak from 280 to 700 K is observed in the TPD spectrum of  $m/z = 31$ , which may be assigned to alcohols formation. However, because of the small signal, it is hard to determine which kind of alcohol it is.

With increasing irradiation time, the desorbed  $\text{CH}_3\text{CHO}$  signal, depicted in Figure 2A, decreases monotonically, suggesting that the  $\text{CH}_3\text{CHO}$  molecules on A- $\text{TiO}_2(101)$  are photodesorbed or reacted to produce 2-butanone. Concomitant to the decrease of the  $\text{CH}_3\text{CHO}$  TPD peak, the 2-butanone product at 320 K appears in TPD spectra of  $m/z = 43$

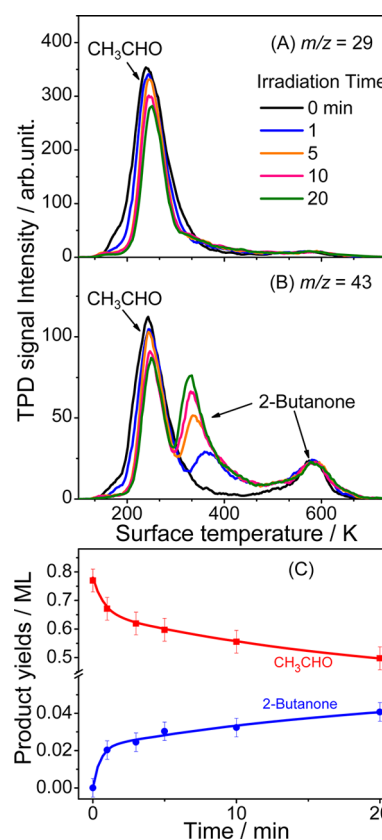
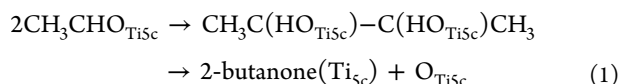


**Figure 2.** A- $\text{TiO}_2(110)$  surface was dosed with 0.8 ML of  $\text{CH}_3\text{CHO}$  at 100 K. (A) Typical TPD spectra collected at  $m/z = 29$  ( $\text{CHO}^+$ ) following different laser irradiation times.  $\text{CHO}^+$  is formed by dissociative ionization of the desorbed parent  $\text{CH}_3\text{CHO}$  molecule in the electron-bombardment ionizer. (B) Typical TPD spectra collected at  $m/z = 43$  ( $\text{C}_2\text{H}_2\text{O}^+$ ) following different laser irradiation times.  $m/z = 43$  ( $\text{C}_2\text{H}_2\text{O}^+$ ) signal mainly has two components: the ion-fragment signals of the parent  $\text{CH}_3\text{CHO}$  molecule and the parent 2-butanone product. (C) Yields of  $\text{CH}_3\text{CHO}$  and 2-butanone as a function of irradiation time following adsorption of 0.8 ML of  $\text{CH}_3\text{CHO}$  on the A- $\text{TiO}_2(101)$  surface at 100 K, derived from data in A and B.

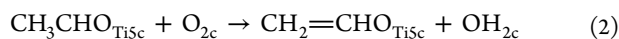
and increases in magnitude as laser irradiation time increases (Figure 2B), while the 2-butanone product desorbed at 580 K keeps unchanged. Compared to our previous study on thermal carbonyl coupling of CH<sub>3</sub>CHO to produce 2-butanone with surplus O atoms left on the highly reduced R-TiO<sub>2</sub>(110) surface,<sup>10</sup> the 2-butanone product detected after irradiation is likely formed via carbonyl coupling of CH<sub>3</sub>CHO with an O atom left on the surface.

To evaluate the importance of 2-butanone formation on A-TiO<sub>2</sub>(101), the yields of CH<sub>3</sub>CHO and 2-butanone products (at 320 K) as a function of UV light irradiation time have been calculated and plotted in Figure 2C. After 20 min irradiation, 0.27 ML of CH<sub>3</sub>CHO is depleted and about 0.04 ML of 2-butanone is produced, indicating that the 2-butanone formation does not possibly occur via surface oxygen vacancy-assisted carbonyl coupling of CH<sub>3</sub>CHO on the A-TiO<sub>2</sub>(101) surface with a low concentration of surface point defects. As mentioned above, the McMurry reaction, aldol condensation, and ketonization are important routes in which aldehydes (or carbonyl containing species) can be converted into longer chain molecules. On TiO<sub>2</sub> and CeO<sub>2</sub> surfaces, ketonization of carboxylate-type species with the evolution of CO<sub>2</sub> and H<sub>2</sub>O has only been achieved; thus, direct ketonization of CH<sub>3</sub>CHO to 2-butanone is not possible.

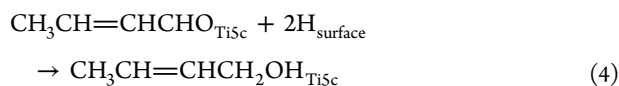
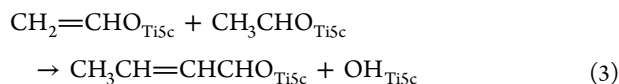
The other two mechanisms are possible. For the McMurry reaction,<sup>15</sup> the pinacolate intermediate (CH<sub>3</sub>-C(HOTi<sub>5c</sub>)-C(HOTi<sub>5c</sub>)-CH<sub>3</sub>) may be formed by carbonyl coupling of CH<sub>3</sub>CHO first and then the intermediate maybe undergoes deoxygenation of O atoms to yield 2-butanone products



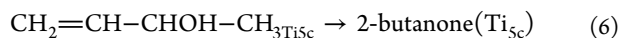
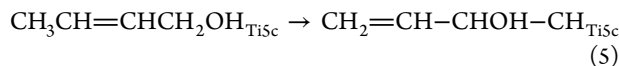
For the aldol condensation route, one CH<sub>3</sub>CHO<sub>Ti5c</sub> molecule isomerizes to enolate first<sup>14</sup>



and then crotonyl alcohol and crotonaldehyde can be formed



As shown in Figure 1, before irradiation, obvious crotonaldehyde product was produced during the TPD process, while no signal of crotonyl alcohol was detected. After irradiation, the increased TPD signal at  $m/z = 31$  indicates that crotonyl alcohol may be formed during UV irradiation. On the basis of early studies in solutions,<sup>32–35</sup> crotonyl alcohol could isomerize to  $\alpha$ -methyl allyl alcohol first and further isomerize to 2-butanone



In this work, photoinduced isomerization of crotonyl alcohol on A-TiO<sub>2</sub>(101) maybe occurs. Later, the possible mechanisms will be discussed in detail.

After 20 min irradiation, 0.27 ML of CH<sub>3</sub>CHO is depleted and about 0.04 ML of 2-butanone is produced. The other 0.19

ML of CH<sub>3</sub>CHO may be desorbed or reacted to produce other easily photodesorbed products during UV irradiation. To identify other possible reaction channels, the time-of-flight (TOF) method was employed to detect possible products directly ejected from the CH<sub>3</sub>CHO-covered surface using a third harmonic (266 nm) of a femtosecond laser (Coherent Co., 1 kHz, 70 fs, 70 mW/cm<sup>2</sup>). As shown in Figure 3, TOF

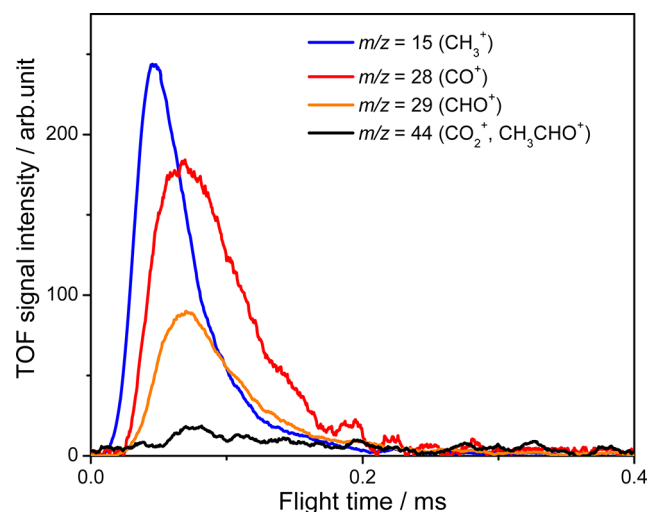
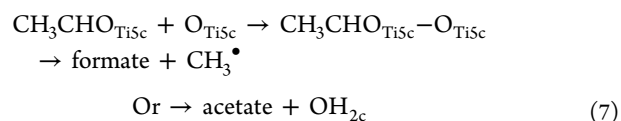
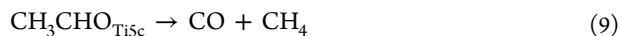
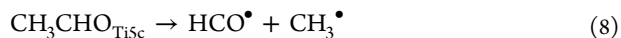


**Figure 3.** TOF signals of  $m/z = 15$  (CH<sub>3</sub><sup>+</sup>), 28 (CO<sup>+</sup>), 29 (CHO<sup>+</sup>), and 44 (CO<sub>2</sub><sup>+</sup>, CH<sub>3</sub>CHO<sup>+</sup>) yield from the A-TiO<sub>2</sub>(101) surfaces prepared with 0.8 ML of adsorbed CH<sub>3</sub>CHO. TOF signals were accumulated for 20 min during 266 nm irradiation.

signals of  $m/z = 15$  (CH<sub>3</sub><sup>+</sup>), 28 (CO<sup>+</sup>), 29 (CHO<sup>+</sup>), and 44 (CO<sub>2</sub><sup>+</sup>, CH<sub>3</sub>CHO<sup>+</sup>) were detected. A previous study of CH<sub>3</sub>CHO photochemistry on preoxidized R-TiO<sub>2</sub>(110)<sup>36</sup> by Henderson and co-workers found that the decomposition of CH<sub>3</sub>CHO with UV irradiation undergoes ejection of a methyl radical (CH<sub>3</sub><sup>•</sup>) into the gas phase and conversion of the surface-bound fragment into formate via a CH<sub>3</sub>CHO–O complex



Direct dissociation of CH<sub>3</sub>CHO to produce CH<sub>3</sub><sup>•</sup> and HCO<sup>•</sup> radicals or CH<sub>4</sub> and CO could be also achieved at 266 nm irradiation<sup>37</sup>



Here, the much larger TOF signals of  $m/z = 15$  and 28 (Figure 3) suggest that the three decomposition channels are all possible. The little TOF signal of  $m/z = 44$  implies that a small amount of CH<sub>3</sub>CHO is desorbed during irradiation. Although the decomposition of CH<sub>3</sub>CHO on A-TiO<sub>2</sub>(101) may occur through three or even more parallel reaction channels, the formation of 2-butanone via photoinduced carbonyl coupling of CH<sub>3</sub>CHO is very efficient.

**Photoinduced Carbonyl Coupling of CH<sub>3</sub>CH<sub>2</sub>CHO.** In order to further confirm whether photoinduced carbonyl coupling of aldehydes to ketones on the surface is universal, photolysis of two other aldehydes (CH<sub>3</sub>CH<sub>2</sub>CHO, PhCHO)



on A-TiO<sub>2</sub>(101) was also carried out. As shown in Figure 4, TPD spectra of various mass traces with a 0.7 ML of

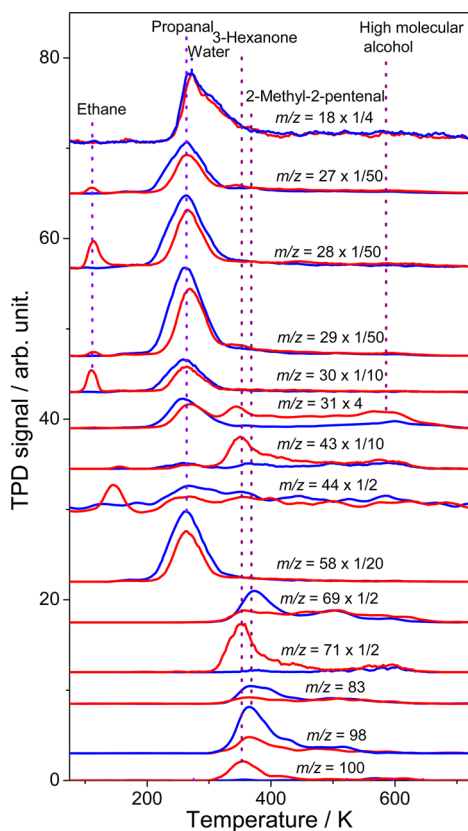
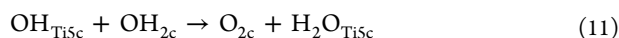
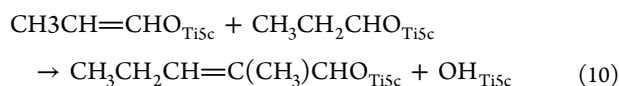
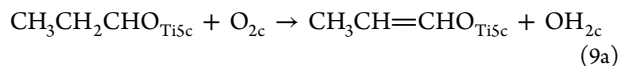


**Figure 4.** TPD spectra acquired at  $m/z = 18$  ( $\text{H}_2\text{O}^+$ ), 27 ( $\text{C}_2\text{H}_3^+$ ), 28 ( $\text{CO}^+$ ,  $\text{C}_2\text{H}_4^+$ ), 29 ( $\text{CHO}^+$ ), 31 ( $\text{CH}_3\text{O}^+$ ), 43 ( $\text{C}_2\text{H}_3\text{O}^+$ ,  $\text{C}_3\text{H}_7^+$ ), 44 ( $\text{C}_2\text{H}_4\text{O}^+$ ,  $\text{C}_3\text{H}_8^+$ ), 58 ( $\text{C}_3\text{H}_6\text{O}^+$ ), 69 ( $\text{C}_4\text{H}_8\text{O}^+$ ), 71 ( $\text{C}_4\text{H}_9\text{O}^+$ ), 83 ( $\text{C}_5\text{H}_7\text{O}^+$ ), 98 ( $\text{C}_6\text{H}_{10}\text{O}^+$ ), and 100 ( $\text{C}_6\text{H}_{12}\text{O}^+$ ) after irradiating the 0.7 ML of  $\text{CH}_3\text{CH}_2\text{CHO}$ -covered A-TiO<sub>2</sub>(101) surface 0 (blue) and 20 min (red).

$\text{CH}_3\text{CH}_2\text{CHO}$ -covered A-TiO<sub>2</sub>(101) surface were measured as well. Before irradiation, three desorption peaks at 260, 270, and 365 K are observed (blue line). The significant desorption peak at 260 K ( $m/z = 27, 28, 29, 30, 58$ ) is assigned to  $\text{CH}_3\text{CH}_2\text{CHO}$  desorption from the  $\text{Ti}_{5c}$  sites. Considering the detection efficiencies of different masses of our quadrupole mass spectrometer and other possible mass traces, 2-methyl-2-pentenal ( $\text{CH}_3\text{CH}_2\text{CH}=\text{C}(\text{CH}_3)\text{CHO}$ ) formation (365 K peak) is identified by comparison of the fragmentation pattern of the evolving species to that given in the NIST database. Similar to the crotonaldehyde formation on the A-TiO<sub>2</sub>(101) surface, 2-methyl-2-pentenal ( $\text{CH}_3\text{CH}_2\text{CH}=\text{C}(\text{CH}_3)\text{CHO}$ ) can be produced via aldol condensation of  $\text{CH}_3\text{CH}_2\text{CHO}$

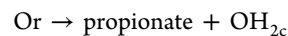
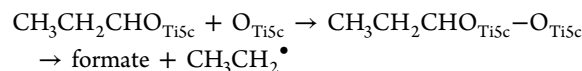


The desorption peak at 270 K ( $m/z = 18$ ) is assigned to the desorption of molecularly adsorbed  $\text{H}_2\text{O}$  at the  $\text{Ti}_{5c}$  sites ( $\text{H}_2\text{O}_{\text{Ti5c}}$ ). The coverage of  $\text{H}_2\text{O}_{\text{Ti5c}}$  is about 0.06 ML.

However, the ratio of  $\text{H}_2\text{O}$  in our  $\text{CH}_3\text{CH}_2\text{CHO}$  sample is less than 0.5%. This clearly demonstrates that the reaction routes (reactions 9–11) for aldol condensation of  $\text{CH}_3\text{CH}_2\text{CHO}$  are reasonable, while the low desorption temperature of  $\text{H}_2\text{O}$  indicates that the aldol condensation of  $\text{CH}_3\text{CH}_2\text{CHO}$  occurs very easily on A-TiO<sub>2</sub>(101). The little signal of the 365 K peak at  $m/z = 31$  suggests that little crotyl alcohol or other alcohols is formed.

After 20 min irradiation, three new peaks at 110 ( $m/z = 27, 28, 29$ ), 148 ( $m/z = 44$ ), and 345 K ( $m/z = 43, 71$ , and 100) appear. Similar to 2-butanone formation from photo-induced carbonyl coupling of  $\text{CH}_3\text{CHO}$  on A-TiO<sub>2</sub>(101), the 345 K peak may be assigned to 3-hexanone, while the respective relative intensities of the 345 K product at  $m/z = 43, 71$ , and 100 (1:0.286:0.071) is the same as that of 3-hexanone (1:0.284:0.072 in Figure S2), demonstrating that photoinduced carbonyl coupling of  $\text{CH}_3\text{CH}_2\text{CHO}$  also occurs on this surface. Considering the detection efficiencies of different masses of our quadrupole mass spectrometer and other possible mass traces, the 110 K peak corresponds to ethane ( $\text{C}_2\text{H}_6$ ) production, which clarifies the direct photodissociation channels of  $\text{CH}_3\text{CH}_2\text{CHO}$  on A-TiO<sub>2</sub>(101).<sup>38</sup> The 148 K peak is mainly detected in the TPD of  $m/z = 44$ , demonstrating that the peak corresponds to  $\text{CO}_2$  desorption.

As UV irradiation time increases, the desorbed  $\text{CH}_3\text{CH}_2\text{CHO}$  and 2-methyl-2-pentenal signals (Figure 5A) decrease monotonically. The 3-hexanone product at 345 K appears and increases in magnitude in the TPD spectra of  $m/z = 43$  (Figure 5B). After 40 min irradiation, 0.3 ML of  $\text{CH}_3\text{CH}_2\text{CHO}$  is consumed and about 0.06 ML of 3-hexanone is produced (Figure 5C). The other 0.18 ML of  $\text{CH}_3\text{CH}_2\text{CHO}$  may be desorbed or decomposed through the pathways that are similar to those of  $\text{CH}_3\text{CHO}$ . The  $\text{C}_2\text{H}_6$  production clarifies the existence of direct photodissociation channels of  $\text{CH}_3\text{CH}_2\text{CHO}$  on A-TiO<sub>2</sub>(101).<sup>38</sup> Similar to the surface  $\text{O}_{\text{Ti5c}}$  atoms assisted photodecomposition of  $\text{CH}_3\text{CHO}$  on A-TiO<sub>2</sub>(101), the surface  $\text{O}_{\text{Ti5c}}$  atoms assisted photodecomposition of  $\text{CH}_3\text{CH}_2\text{CHO}$  is also possible



(12)

**Photoinduced Carbonyl Coupling of PhCHO.** Photolysis of PhCHO on A-TiO<sub>2</sub>(101) was further investigated. As shown in Figure 6A, PhCHO (parent ion  $m/z = 106$ ) desorbs in three features: (1) a high-temperature peak at ~480 K, (2) a middle-temperature peak at ~310 K, and (3) a low-temperature shoulder at 210 K. The desorption feature is similar to that of PhCHO observed on R-TiO<sub>2</sub>(110).<sup>12</sup> With increasing irradiation time, two new peaks at 430 and 600 K appear in TPD spectra of  $m/z = 105$  and increase significantly (Figure 6B). Considering the detection efficiencies of different masses of our quadrupole mass spectrometer and other possible mass traces (Figure 7), benzyl phenyl ketone [largest ion-fragment  $m/z = 105$  ( $\text{C}_7\text{H}_5\text{O}^+$ )] is identified by comparison of the fragmentation pattern of the evolving species to that given in the NIST database. Unfortunately, because of the low vapor pressure of benzyl phenyl ketone, a separate TPD experiment of benzyl phenyl ketone on A-TiO<sub>2</sub>(101) could not be accomplished to calculate the yield of benzyl phenyl ketone as well as the yield of benzyl phenyl ketone.

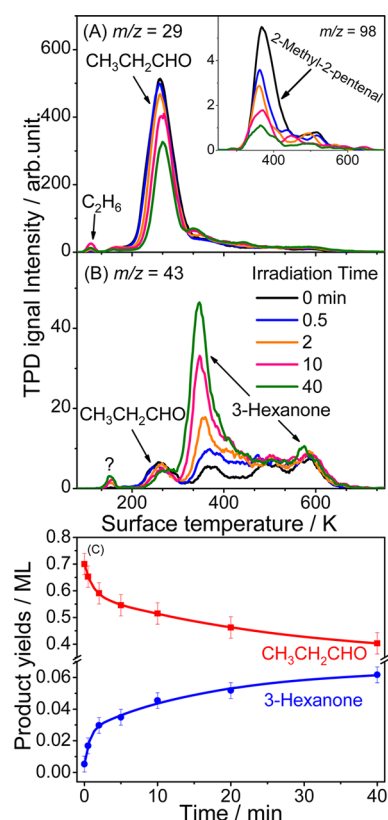


**Figure 5.** A- $\text{TiO}_2(110)$  surface was dosed with 0.7 ML of  $\text{CH}_3\text{CH}_2\text{CHO}$  at 100 K. (A) Typical TPD spectra collected at  $m/z = 29$  ( $\text{C}_2\text{H}_5^+$ ,  $\text{CHO}^+$ ) following different laser irradiation times.  $\text{C}_2\text{H}_5^+$  and  $\text{CHO}^+$  are formed by dissociative ionization of the desorbed parent  $\text{CH}_3\text{CHO}$  molecule in the electron-bombardment ionizer. (B) Typical TPD spectra collected at  $m/z = 43$  ( $\text{C}_2\text{H}_5\text{O}^+$ ) following different laser irradiation times. The  $m/z = 43$  ( $\text{C}_2\text{H}_5\text{O}^+$ ) signal mainly has two components: the ion-fragment signals of the parent  $\text{CH}_3\text{CH}_2\text{CHO}$  molecule and the parent 3-hexanone product; the intensity of the TPD peak of other species are too small to be assigned. (C) Yields of  $\text{CH}_3\text{CH}_2\text{O}$  and 3-hexanone as a function of irradiation time following adsorption of 0.7 ML of  $\text{CH}_3\text{CH}_2\text{CHO}$  on the A- $\text{TiO}_2(101)$  surface at 100 K, derived from data in A and B.

## DISCUSSION

Although the formation of ketones involves several steps of photoinduced C–H bond scission, no  $\text{H}_2$  is observed during both UV irradiation and the TPD process. There may be two reasons for no evidence of  $\text{H}_2$  desorption. First, the  $\text{H}_2$  background in the detecting zone is still high; it is not easy for us to detect molecular  $\text{H}_2$  desorption during UV irradiation using the TOF method. Second, the formation of ketones will leave O atoms on the surface; H atoms can be depleted by the O atoms to produce  $\text{H}_2\text{O}$ . Thus, there is no obvious evidence of molecular  $\text{H}_2$  desorption.

As shown in Figure 5, 3-hexanone formation seems to be related with the 2-methyl-2-pentenal depletion, while on the 0.8 ML of  $\text{CH}_3\text{CHO}$ -covered A- $\text{TiO}_2(110)$  surface, the 2-butanone production seems also to be related with the crotonaldehyde depletion. As discussed above, 2-butanone may be formed through crotonaldehyde hydrogenation and isomerization processes. However, with the similar hydrogenation and isomerization processes, the 3-hexanone product cannot be formed from 2-methyl-2-pentenal. Thus, the mechanism for ketones formation from aldehydes via ketenes is impossible.

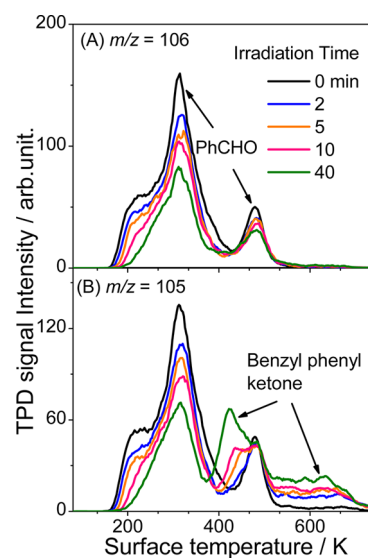


**Figure 6.** A- $\text{TiO}_2(110)$  surface was dosed with 0.7 ML of PhCHO at 100 K. (A) Typical TPD spectra collected at  $m/z = 106$  ( $\text{C}_7\text{H}_6\text{O}^+$ ) following different laser irradiation times. (B) Typical TPD spectra collected at  $m/z = 105$  ( $\text{C}_7\text{H}_5\text{O}^+$ ) following different laser irradiation times. The  $m/z = 105$  ( $\text{C}_7\text{H}_5\text{O}^+$ ) signal mainly has two components: the parent ion signal of PhCHO and the ion-fragment signals of the parent benzyl phenyl ketone molecule product.

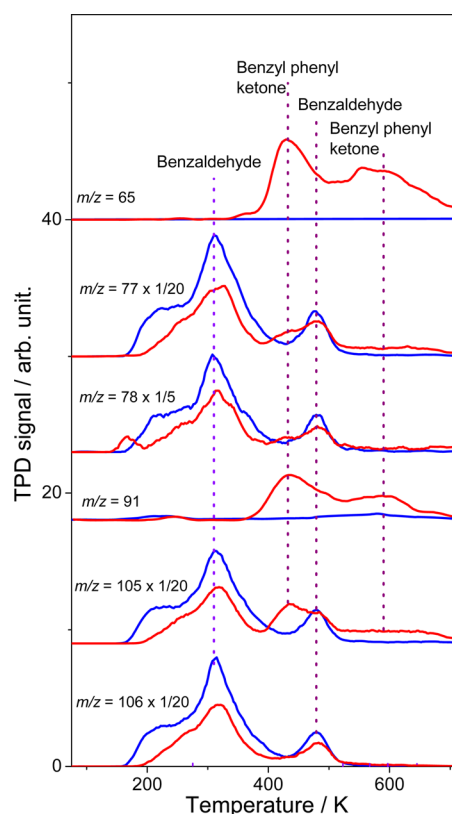


**Figure 7.** TPD spectra acquired at  $m/z = 65$  ( $\text{C}_5\text{H}_5^+$ ), 77 ( $\text{C}_6\text{H}_5^+$ ), 78 ( $\text{C}_6\text{H}_6^+$ ), 91 ( $\text{C}_7\text{H}_7^+$ ), 105 ( $\text{C}_7\text{H}_5\text{O}^+$ ), and 106 ( $\text{C}_7\text{H}_6\text{O}^+$ ) after irradiating the 0.7 ML of PhCHO-covered A- $\text{TiO}_2(101)$  surface 0 (blue) and 20 min (red).

According to the mechanism of the McMurry reaction and previous studies of aldehydes on rutile  $\text{TiO}_2$  surfaces,<sup>10–24</sup> surface low-valent Ti sites play an important role for carbonyl

coupling reaction of aldehydes. However, a recent study of reductive C=C coupling of benzaldehyde on the oxidized R-TiO<sub>2</sub>(110) surface by Benz and co-workers<sup>12</sup> demonstrated that the Ti interstitials at the subsurface region play an important role in the McMurry-type coupling of PhCHO. For the reduced A-TiO<sub>2</sub>(101) surface used in the experiment, intrinsic defects reside (Ti interstitials) predominantly in the subsurface region with a substantially lower formation energy than at surface sites.<sup>31</sup> Therefore, the 2-butanone, 3-hexanone, and 2-methyl-2-pentenal products formed via carbonyl coupling reaction of aldehydes on the Ti<sub>5c</sub> sites of the A-TiO<sub>2</sub>(101) surface without irradiation are most likely to be driven by the Ti interstitials in the subsurface region. Upon photoexcitation, the low-valent Ti sites (Ti<sup>3+</sup>) on the surface can be produced via reduction of surface Ti<sub>5c</sub> (Ti<sup>4+</sup>) sites with excited electrons. Then part of the aldehyde molecules on the Ti<sup>3+</sup> sites are likely to react with adjacent aldehyde molecules to form the pinacolate intermediate (R-C(HO<sub>Ti5c</sub>)-C(HO<sub>Ti5c</sub>)-R, R = CH<sub>3</sub>, CH<sub>3</sub>CH<sub>2</sub>, Ph) (Figure 8). Finally, the ketone products

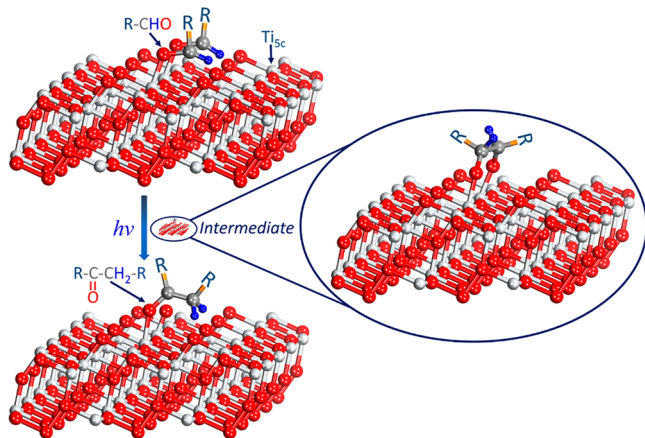
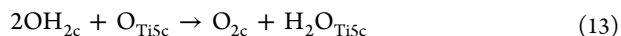


**Figure 8.** Schematic model for photoinduced carbonyl coupling of aldehydes on A-TiO<sub>2</sub>(101).

may be formed from the pinacolate intermediates during UV irradiation or during the TPD process. However, the desorption temperatures of ketone products (2-butanone and 3-hexanone) produced with UV irradiation are about 200 K lower than that observed without irradiation, implying that the formation of the ketone products is most likely to be driven by charge carriers generated during UV irradiation and not by heat during the TPD process.

Without irradiation, the 2-methyl-2-pentenal product is formed via aldol condensation of CH<sub>3</sub>CH<sub>2</sub>CHO with the evolution of H<sub>2</sub>O<sub>Ti5c</sub>. After irradiating the 0.7 ML of CH<sub>3</sub>CH<sub>2</sub>CHO-covered A-TiO<sub>2</sub>(110) surface for 20 min, the 2-methyl-2-pentenal product via aldol condensation decreases significantly on the surface (Figure 5), which will lead to the decrease of H<sub>2</sub>O<sub>Ti5c</sub> formation. However, the amount of H<sub>2</sub>O<sub>Ti5c</sub> produced on the surface keeps unchanged; the H<sub>2</sub>O absolutely does not come from the CH<sub>3</sub>CH<sub>2</sub>CHO sample. As the 3-hexanone product is produced, surplus O atoms will be left on the Ti<sub>5c</sub> sites of the surface (O<sub>Ti5c</sub>), while through reaction 12, part of the O<sub>Ti5c</sub> atoms can be depleted with the evolution of OH<sub>2c</sub>. Further, the OH<sub>2c</sub> groups formed via reaction 12 will react with the O<sub>Ti5c</sub> atoms to produce H<sub>2</sub>O<sub>Ti5c</sub>



Thus, the H<sub>2</sub>O<sub>Ti5c</sub> may keep unchanged as the amount of H<sub>2</sub>O<sub>Ti5c</sub> produced via aldol condensation of CH<sub>3</sub>CH<sub>2</sub>CHO decreases. Besides, our previous studies of photoinduced decomposition of formaldehyde (CH<sub>2</sub>O) on R-TiO<sub>2</sub>(110)<sup>39</sup> found that bridging oxygen atoms are intimately involved in the photoinduced decomposition of CH<sub>2</sub>O on R-TiO<sub>2</sub>(110). On A-TiO<sub>2</sub>(101), O<sub>2c</sub> atoms may be also possibly involved in the photoinduced decomposition of aldehydes.

## SUMMARY

In summary, our experimental results show the photoinduced carbonyl coupling reaction of aldehydes occurs on A-TiO<sub>2</sub>(101) efficiently,  $2\text{R}-\text{CHO}_{\text{Ti5c}} \rightarrow \text{R}-\text{CH}_2-\text{CO}-\text{R}(\text{Ti}_{5c}) + \text{O}_{\text{Ti5c}}$ . A possible mechanism has thus been derived for the oxidation of the simple aldehyde precursors on a model TiO<sub>2</sub> surface to build more complex molecules. The observation that ketone formation is promoted by light at low temperatures further demonstrates the utility of TiO<sub>2</sub> as a photocatalyst for synthetic reactions, unlike noble metals which typically act as thermal catalysts.

## ASSOCIATED CONTENT

### Supporting Information

The Supporting Information is available free of charge on the ACS Publications website at DOI: 10.1021/acs.jpcc.6b02713.

TPD spectra acquired at a variety of different mass-to-charge ratios after 0.22 ML of 2-butanone was adsorbed on A-TiO<sub>2</sub>(101); TPD spectra acquired at a variety of different mass-to-charge ratios after 0.14 ML of 3-hexanone was adsorbed on A-TiO<sub>2</sub>(101) (PDF)

## AUTHOR INFORMATION

### Corresponding Authors

\*E-mail: guoqing@dicp.ac.cn.

\*E-mail: xmyang@dicp.ac.cn.

### Author Contributions

<sup>†</sup>Z.G. and X.C. contributed equally to this work.

### Notes

The authors declare no competing financial interest.

## ACKNOWLEDGMENTS

This work was supported by the National Science Foundation of China (21403224) and the Chinese Ministry of Science and Technology (2013CB834605), the Youth Innovation Promotion Association CAS, and the Key Research Program of the Chinese Academy of Sciences.

## REFERENCES

- (1) Fujishima, A.; Honda, K. Electrochemical Photolysis of Water at a Semiconductor Electrode. *Nature* **1972**, *238*, 37–38.
- (2) Chen, X.; Mao, S. S. Titanium Dioxide Nanomaterials: Synthesis, Properties, Modifications, and Applications. *Chem. Rev.* **2007**, *107*, 2891–2959.
- (3) Pang, C. L.; Lindsay, R.; Thornton, G. Chemical Reactions on Rutile TiO<sub>2</sub>(110). *Chem. Soc. Rev.* **2008**, *37*, 2328–2353.
- (4) Diebold, U. The Surface Science of Titanium Dioxide. *Surf. Sci. Rep.* **2003**, *48*, 53–229.
- (5) Hoffmann, M. R.; Martin, S. T.; Choi, W. Y.; Bahnemann, D. W. Environmental Applications of Semiconductor Photocatalysis. *Chem. Rev.* **1995**, *95*, 69–96.
- (6) Thompson, T. L.; Yates, J. T., Jr. Surface Science Studies of the Photoactivation of TiO<sub>2</sub> New Photochemical Processes. *Chem. Rev.* **2006**, *106*, 4428–4453.



- (7) Henderson, M. A. A Surface Science Perspective on  $\text{TiO}_2$  Photocatalysis. *Surf. Sci. Rep.* **2011**, *66*, 185–297.
- (8) Fujishima, A.; Zhang, X.; Tryk, D.  $\text{TiO}_2$  Photocatalysis and Related Surface Phenomena. *Surf. Sci. Rep.* **2008**, *63*, 515–582.
- (9) Bai, J.; Zhou, B. X. Titanium Dioxide Nanomaterials for Sensor Applications. *Chem. Rev.* **2014**, *114*, 10131–10176.
- (10) Yang, W.; Geng, Z.; Xu, C.; Guo, Q.; Dai, D.; Yang, X. Controlled Vacancy-Assisted C–C Couplings of Acetaldehyde on Rutile  $\text{TiO}_2(110)$ . *J. Phys. Chem. C* **2014**, *118*, 27920–27924.
- (11) Benz, L.; Haubrich, J.; Quiller, R. G.; Friend, C. M. Acrolein Coupling on Reduced  $\text{TiO}_2(110)$ : The Effect of Surface Oxidation and the Role of Subsurface Defects. *Surf. Sci.* **2009**, *603*, 1010–1017.
- (12) Benz, L.; Haubrich, J.; Quiller, R. G.; Jensen, S. C.; Friend, C. M. McMurry Chemistry on  $\text{TiO}_2(110)$ : Reductive C=C Coupling of Benzaldehyde Driven by Titanium Interstitials. *J. Am. Chem. Soc.* **2009**, *131*, 15026–15031.
- (13) Idriss, H.; Pierce, K.; Barteau, M. A. Carbonyl Coupling on the Titanium Dioxide  $\text{TiO}_2(001)$  surface. *J. Am. Chem. Soc.* **1991**, *113*, 715–716.
- (14) Idriss, H.; Barteau, M. A. Selectivity and Mechanism Shifts in the Reactions of Acetaldehyde on Oxidized and Reduced  $\text{TiO}_2(001)$  Surfaces. *Catal. Lett.* **1996**, *40*, 147–153.
- (15) McMurry, J. E. Carbonyl-Coupling Reactions Using Low-Valent Titanium. *Chem. Rev.* **1989**, *89*, 1513–1524.
- (16) Dooley, K. M. Catalysis of Acid/Aldehyde/Alcohol Condensations to Ketones. In *Catalysis*; Roberts, J. J. S. A. G. W., Ed.; The Royal Society of Chemistry: Cambridge, 2004; pp 293–319.
- (17) Rekoske, J. E.; Barteau, M. A. Kinetics, Selectivity, and Deactivation in the Aldol Condensation of Acetaldehyde on Anatase Titanium Dioxide. *Ind. Eng. Chem. Res.* **2011**, *50*, 41–51.
- (18) Singh, M.; Zhou, N.; Paul, D. K.; Klabunde, K. J. IR Spectral Evidence of Aldol Condensation: Acetaldehyde Adsorption over  $\text{TiO}_2$  Surface. *J. Catal.* **2008**, *260*, 371–379.
- (19) Raskó, J.; Kiss, J. Adsorption and Surface Reactions of Acetaldehyde on  $\text{TiO}_2$ ,  $\text{CeO}_2$  and  $\text{Al}_2\text{O}_3$ . *Appl. Catal., A* **2005**, *287*, 252–260.
- (20) Idriss, H.; Kim, K. S.; Barteau, M. A. Carbon-Carbon Bond Formation via Aldolization of Acetaldehyde on Single Crystal and Polycrystalline  $\text{TiO}_2$  Surfaces. *J. Catal.* **1993**, *139*, 119–133.
- (21) Rekoske, J. E.; Barteau, M. A. Competition between Acetaldehyde and Crotonaldehyde during Adsorption and Reaction on Anatase and Rutile Titanium Dioxide. *Langmuir* **1999**, *15*, 2061–2070.
- (22) Luo, S.; Falconer, J. L. Aldol Condensation of Acetaldehyde to form High Molecular Weight Compounds on  $\text{TiO}_2$ . *Catal. Lett.* **1999**, *57*, 89–93.
- (23) Luo, S.; Falconer, J. L. Acetone and Acetaldehyde Oligomerization on  $\text{TiO}_2$  Surfaces. *J. Catal.* **1999**, *185*, 393–407.
- (24) Idriss, H.; Pierce, K. G.; Barteau, M. A. Synthesis of Stilbene from Benzaldehyde by Reductive Coupling on  $\text{TiO}_2(001)$  Surfaces. *J. Am. Chem. Soc.* **1994**, *116*, 3063–3074.
- (25) Idriss, H.; Diagne, C.; Hindermann, J. P.; Kiennemann, A.; Barteau, M. Reactions of Acetaldehyde on  $\text{CeO}_2$  and  $\text{CeO}_2$ -Supported Catalysts. *J. Catal.* **1995**, *155*, 219–237.
- (26) Kamimura, Y.; Sato, S.; Takahashi, R.; Sodesawa, T.; Akashi, T. Synthesis of 3-Pentanone from 1-Propanol over  $\text{CeO}_2\text{--Fe}_2\text{O}_3$  Catalysts. *Appl. Catal., A* **2003**, *252*, 399–410.
- (27) Kobune, M.; Sato, S.; Takahashi, R. J. Mol. Surface-Structure Sensitivity of  $\text{CeO}_2$  for Several Catalytic Reactions. *J. Mol. Catal. A: Chem.* **2008**, *279*, 10–19.
- (28) Kim, K. S.; Barteau, M. A. Structure and Composition Requirements for Deoxygenation, Dehydration, and Ketonization Reactions of Carboxylic Acids on  $\text{TiO}_2(001)$  Single-Crystal Surfaces. *J. Catal.* **1990**, *125*, 353–375.
- (29) Kim, K. S.; Barteau, M. A. Structural Dependence of the Selectivity of Formic Acid Decomposition on Faceted Titania (001) Surfaces. *Langmuir* **1990**, *6*, 1485–1488.
- (30) Ren, Z.; Guo, Q.; Xu, C.; Yang, W.; Xiao, C.; Dai, D.; Yang, X. Surface Photocatalysis-TPD Spectrometer for Photochemical Kinetics. *Chin. J. Chem. Phys.* **2012**, *25*, 507–512.
- (31) He, Y.; Dulub, O.; Cheng, H.; Selloni, A.; Diebold, U. Evidence for the Predominance of Subsurface Defects on Reduced Anatase  $\text{TiO}_2(101)$ . *Phys. Rev. Lett.* **2009**, *102*, 106105.
- (32) Young, W. G.; Franklin, J. S. The Acid-Catalyzed Isomerization of  $\alpha$ - and cis- and trans- $\gamma$ -Methylallyl Alcohols. *J. Am. Chem. Soc.* **1966**, *88*, 785–790.
- (33) Arévalo, M. C.; Rodríguez, J. L.; Castro-Luna, A. M.; Pastor, E. Adsorption, oxidation and reduction of crotyl alcohol on platinum: A DEMS and in situ FTIRS study. *Electrochim. Acta* **2006**, *51*, 5365–5375.
- (34) Van der Drift, R. C.; Sprengers, J. W.; Bouwman, E.; Mul, W. P.; Kooijman, H.; Spek, A. L.; Drent, E. Ruthenium-Catalyzed Isomerization of Allylic Alcohols: Oxidation State Determines Resistance Against Diene Inhibition. *Eur. J. Inorg. Chem.* **2002**, *2002*, 2147–2155.
- (35) Bianchini, C.; Meli, A.; Oberhauser, W. Isomerization of Allylic Alcohols to Carbonyl Compounds by Aqueous-Biphase Rhodium Catalysis. *New J. Chem.* **2001**, *25*, 11–12.
- (36) Zehr, R. T.; Henderson, M. A. Acetaldehyde Photochemistry on  $\text{TiO}_2(110)$ . *Surf. Sci.* **2008**, *602*, 2238–2249.
- (37) Shubert, V. A.; Pratt, S. T. Photodissociation of Acetaldehyde and the Absolute Photoionization Cross Section of  $\text{HCO}$ . *J. Phys. Chem. A* **2010**, *114*, 11238–11243.
- (38) Chen, Y.; Zhu, L. The Wavelength Dependence of the Photodissociation of Propionaldehyde in the 280–330 nm Region. *J. Phys. Chem. A* **2001**, *105*, 9689–9696.
- (39) Xu, C.; Yang, W.; Guo, Q.; Dai, D.; Minton, T. K.; Yang, X. Photoinduced Decomposition of Formaldehyde on a  $\text{TiO}_2(110)$  Surface, Assisted by Bridge-Bonded Oxygen Atoms. *J. Phys. Chem. Lett.* **2013**, *4*, 2668–2673.